Soft Matter

www.rsc.org/softmatter

Volume 7 | Number 5 | 7 March 2011 | Pages 1545–2164

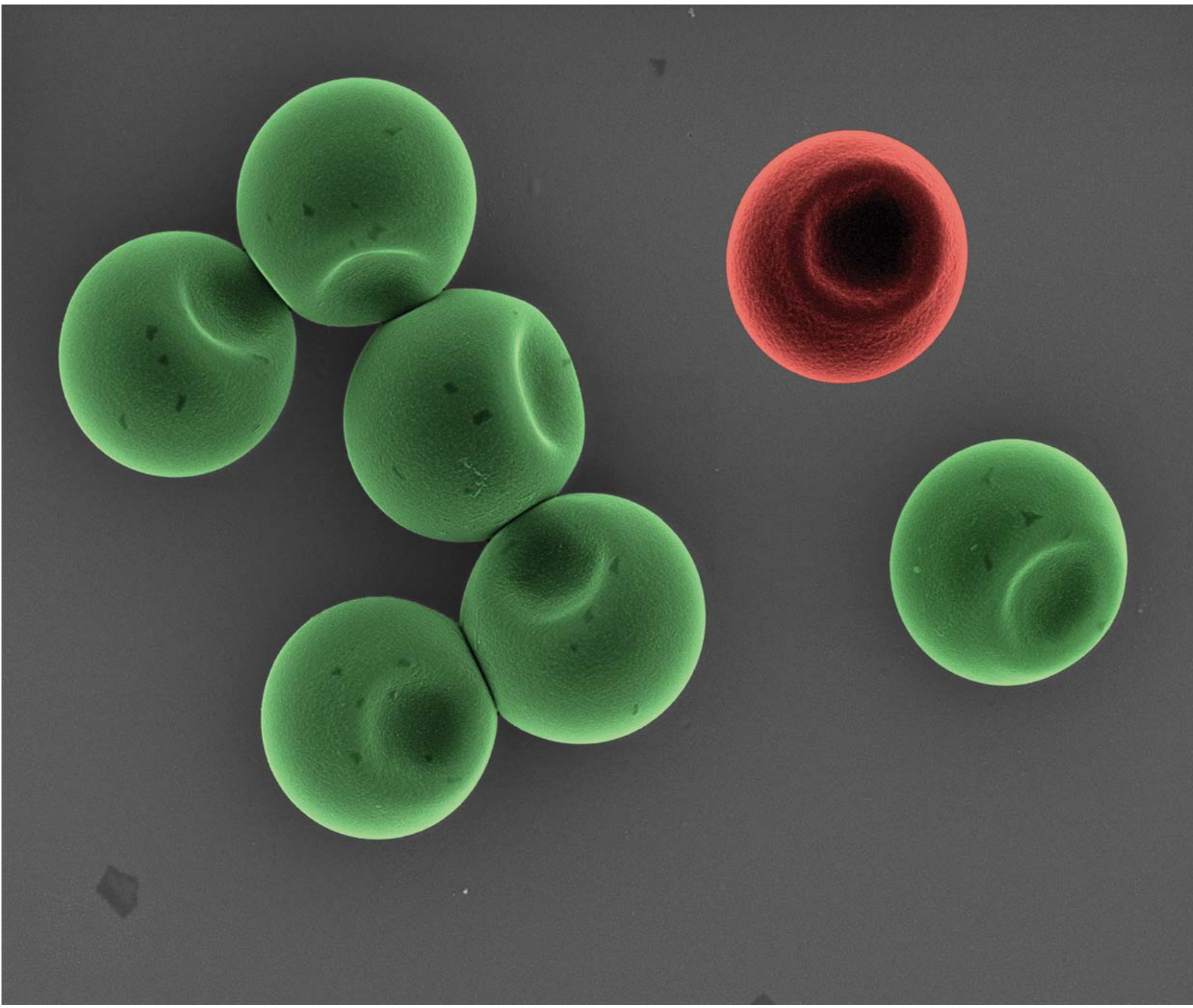

ISSN 1744-683X

RSC Publishing

COMMUNICATION
Stefano Sacanna *et al.*
Lock and key colloids through polymerization-induced buckling of monodisperse silicon oil droplets

1744-683X(2011)7:5;1-K

Lock and key colloids through polymerization-induced buckling of monodisperse silicon oil droplets

Stefano Sacanna,*[a] William T. M. Irvine,[a] Laura Rossi[b] and David J. Pine[a]

Received 7th October 2010, Accepted 11th November 2010
DOI: 10.1039/c0sm01125h

We have developed a new simple method to fabricate bulk amounts of colloidal spheres with well defined cavities from monodisperse emulsions. Herein, we describe the formation mechanism of "reactive" silicon oil droplets that deform to reproducible shapes *via* a polymerization-induced buckling instability. Owing to their unique shape, the resulting particles can be successfully used as colloidal building blocks in the assembly of composite clusters *via* "lock-and-key" interactions.

Over the past dozen years there has been a significant effort to create new assemblies of colloid crystals with increasingly complex structures. However, colloidal particles are typically spherical and thus interact through highly symmetric potentials, which limits their self assembly to a few simple crystal structures or to disordered aggregates. By contrast, molecular self assembly, driven by highly directional interactions yields a much greater range of self assembled structures, and thus greater functionality. Taking a cue from molecular self assembly, a significant effort has emerged recently to create colloidal particles with non-spherical shapes. To date, these efforts have focused mainly on using clever physical strategies,[1–6] or by decorating surfaces with "sticky patches" of biological[7,8] or synthetic molecules.[9,10] These efforts have led to the fabrication of remarkably complex three-dimensional structures, especially when coupled with the depletion attraction, which provides a convenient means to tune the attraction between colloidal particles.[11–15] Making anisotropic particles or assemblies has been vexed, however, by the difficulty of producing highly monodisperse anisotropic particles in the large quantities required for applications.[16]

Herein we describe a simple, high yield, synthetic pathway to fabricate monodisperse hybrid silica spheres with well defined cavities in bulk quantities. In addition, the particle morphologies are reproducible and tunable with precision, resulting in particles with a unique shape that are particularly suitable to be used in the architecture of larger composite clusters *via* depletion-driven lock and key interactions.

The starting point of our method are monodisperse silicon oil droplets nucleated *via* a base catalyzed hydrolysis and condensation of 3-methacryloxypropyltrimethoxysilane (TPM). This emulsification procedure was adapted from the method of Obey[17] and consists of a slow hydrolysis of alkoxysilanes to give metastable water-soluble silanols which undergo a rapid condensation reaction when treated with a strong base. If a trialkoxysilane is used (here TPM), the condensation products are branched three-dimensional silsesquioxanes (see Fig. 1) that precipitate out of solution when their equilibrium solubility has been reached.[18] Above a pH of 9, the insoluble siloxanols phase separate as monodisperse oil droplets that grow without coalescing due to a strong negative surface charge that develops from the dissociation of surface silanol groups. A typical zeta potential for the resulting droplets, measured in an aqueous solution of 10mM NaCl at pH of 9, is about −70mV. The exact composition of the oil droplets is set by the solubility of each individual oligomer produced during the course of the hydrolysis and condensation reactions and it is a mixture of siloxanols with different structures and molecular weights.[18] The size of the droplets can be roughly tuned during the nucleation step by adjusting the initial concentration of hydrolyzed monomer and the amount of base used to initiate the polycondensation.[17] A more precise target size is easily reached by growing freshly nucleated droplets with a continuous feed of hydrolyzed monomer. A typical droplet growth rate is of the order

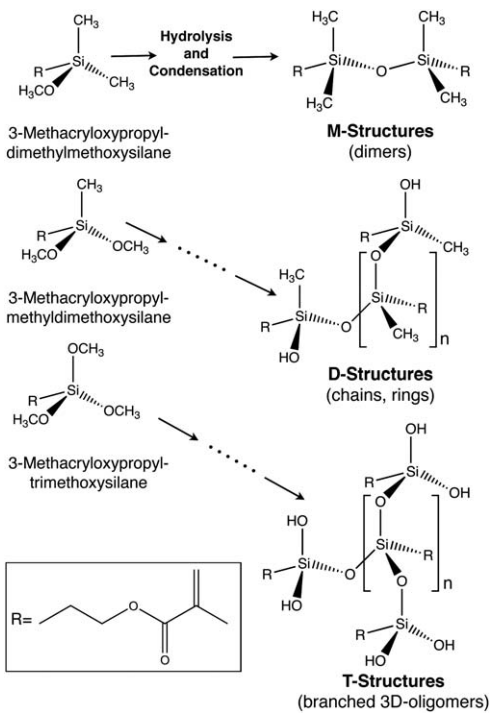

Fig. 1 Scheme illustrating the course of the hydrolysis and condensation reactions for the three types of oils used in our experiments. Depending on the number of methoxysilane moieties in the oil molecule the condensation products might have linear (M-, D-) or branched (T-) structures.

[a]*Center for Soft Matter research, Department of Physics, New York University, 4 Washington Place, New York, New York, 10003, USA. E-mail: s.sacanna@nyu.edu; Tel: +1 (212) 998-8460*
[b]*Van't Hoff Laboratory for Physical and Colloid Chemistry, Debye Institute for Nano-materials Science, Utrecht University, Padualaan 8, 3584 CH Utrecht, The Netherlands*

of 0.4 μm/h which is sufficiently slow to be accurately followed by optical microscopy or light scattering. Monodisperse silicon oil droplets are prepared by first hydrolyzing 5 mL of TPM in 100 mL of deionized water under a vigorous stirring for 24 h. When all the oil is solubilized, 15 mL of this solution are added to 30 mL of aqueous NH_3 0.4M. At this point the mixture rapidly turns turbid as the oil droplets nucleate and grow to a size of about 0.5 μm. The remaining water solution of hydrolyzed TPM is added dropwise until the droplets reach their target size. Their characterization was performed on samples of typically 200 particles, using a Nikon inverted microscope equipped with an 100x oil immersion objective. In the experiments presented herein, we used droplets with an average diameter of 2.5 μm and a typical polydispersity of $\leq$3.5%.

In the next step we create the cavities. Each TPM oligomer that was formed during the condensation reaction carries methacrylate groups that undergo polymerization in the presence of radicals. In our system, the radicals are generated in situ by thermal decomposition of a water soluble radical initiator (potassium persulfate, KPS) which is added to the emulsion at room temperature, to a final concentration of 0.45mM. At the polymerization temperature (75 °C) the KPS decomposes, forming sulfate ion radicals that attack the free TPM oligomers in equilibrium in the water phase. The resulting growing polymers aggregate into new particle nuclei (visible in Fig. 2A) and, most importantly, grow rigid crosslinked shells around the silicon oil droplets. The polymerization reaction continues sustained by a net flow of low molecular weight oligomers that diffuse from the droplets into the water phase until all the soluble species in the droplets have been depleted. The droplets, consumed by the polymerization reaction, deflate driving the shells to deform *via* a buckling instability.[19] This mechanism is analogous to a seeded growth emulsion polymerization[20] where the micron-sized oil droplets act simultaneously as seeds and as reservoirs of reactive species.

We followed the reaction by optical microscopy using a glass capillary filled with oil droplets suspended in the reaction mixture, glued to a heated microscope slide coated with indium tin oxide. The imaging was performed using a 100× air objective to minimize temperature gradients and a thermocouple attached to the capillary with thermal-conductive paste was used to monitor the temperature during the reaction. The experiments (see Fig. 3A) show that the buckling occurs at the KPS decomposition temperature (between 75 and 80 °C), and that the droplets deformation occur for all the droplets simultaneously regardless of their size. At the same temperature, turbidity increases visibly due to the nucleation of secondary particles that are too small to be resolved individually. This is consistent with the hypothesis that the shell and the secondary nucleated particles form immediately after the initial burst of radicals that consumes the soluble oligomers in the water phase, whereas the buckling occurs when low molecular weight oligomers diffuse by osmotic pressure from the droplets to the water phase to restore the equilibrium and sustain the polymerization. As the low molecular weight oligomers are depleted from the droplets, their diffusion time becomes slower because the osmotic driving force decreases and the oil viscosity increases. This is captured in Fig. 3A that shows how the

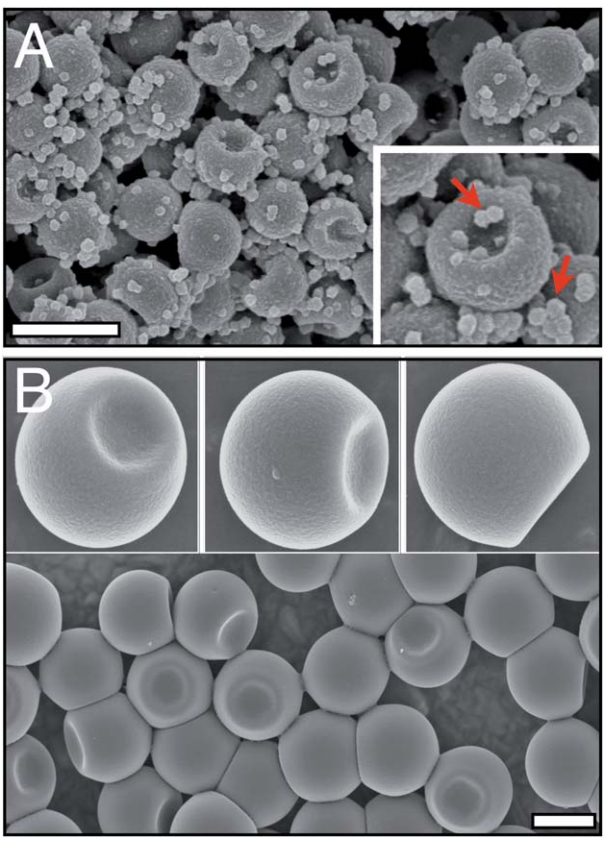

Fig. 2 SEM images of hybrid silica particles prepared through polymerization-induced buckling of monodisperse TPM oil droplets. In (A) the reaction mixture was imaged without purification to show the presence of both polymerized droplets with single dimples and small secondarily nucleated particles (arrows). In (B) the buckled droplets were isolated from the small spheres by sedimentation and redispersion in pure water. Scale bars are 2 μm.

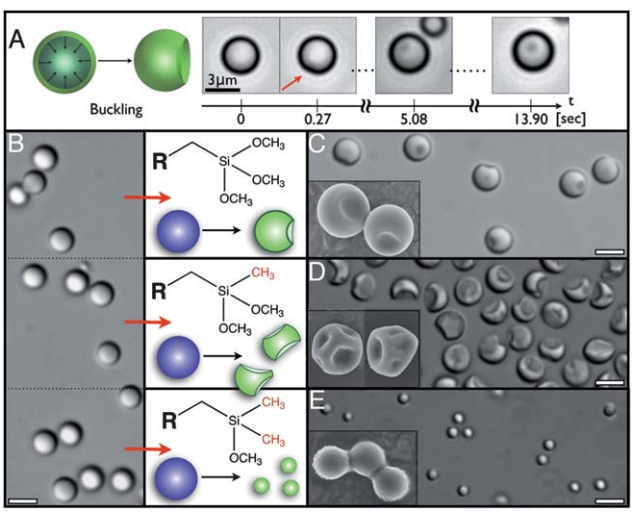

Fig. 3 In (A), snapshots showing a typical deformation dynamic for TPM droplets during the radical polymerization. At the polymerization temperature (75 °C) the droplets shells rapidly buckle forming small dimples that deepens in time to reach their final morphology within 10 s. Depending on the type of monomer used to form the oil droplets (B), the resulting polymerized particles have different morphologies. Upon polymerization, TPM droplets gives particles with smooth surfaces and a single dimple (C). DPM droplets form particles with multiple dimples (D) and MPM droplets shrink homogeneously to form small spherical particles with rough surfaces (E). Scale bars are 3 μm.

initial buckling takes place within our shortest frame acquisition time (270 ms), but it is followed by a slower evolution of the resulting dimple that deepens in time to reach its final morphology after 10 s. The complete polymerization of the droplets occurs during a longer timescale in which the radicals generated in the water phase diffuse into the viscous oil droplets. Typically we observe that a minimum of 2 h is necessary to fully harden the particles to the point that they can be dried and imaged by electron microscopy. After polymerization the density of TPM particles (measured with an Anton Paar density meter, mod. DMA-4500M) increased from 1.045 g/cm^3 (density of the monomer) to 1.228 g/cm^3 (density of the fully polymerized particles). This allows us to infer that the change in the droplet volume is entirely dominated by the fraction of low molecular weight oligomers that leave the droplets during polymerization. From EM pictures of buckled droplets, this fraction was estimated to be of the order of 20%.

If the mechanism that we propose is correct, we would expect that, independently from the radical polymerization, other routes could produce similar droplet deformations, provided that a permeable shell is formed and a following controlled flux matter is established. Thus we attempt to buckle unpolymerized droplets by first growing a thin layer of silica on their surface by hydrolysis and condensation of tetraethoxysilane[21] and then dialyzing the suspension to deplete low molecular weight oligomers from the oil phase. Indeed this produced buckled droplets similar to the polymerized TPM particles of Fig. 3C but with a poor long term colloidal stability in water, probably due to missing ionizable sulfate groups (introduced during the radical polymerization), or to a slow decomposition of the inner liquid core in time. Finally, removing the soluble low molecular weight species by dialysis prior the formation of the droplet outer shell (*e.g.* before initiating the radical polymerization), results in perfectly spherical particles, further confirming the proposed mechanism.

The stiffness of the shell plays a fundamental role on the final particles morphology and it depends on the amount of self-cross linking of the constituent polymer network. We have investigated the effect of the cross linking density on the final particle morphology by progressively replacing the three hydrolyzable methoxy groups in the TPM molecule with non-reactive methyl groups. The resulting 3-(methacryloxypropyl)methyldimethoxy silane (DPM) and 3-(methacryloxypropyl)dimethylmethoxy silane (MPM) monomers (Fig. 1) were then emulsified and polymerized as described earlier for TPM and the morphology of the particles analyzed by microscopy (Fig. 3). A decrease in the surface zeta potential from −74 mV to −38 mV, measured on TPM and MPM emulsion droplets respectively, confirms the presence of a reduced number of methoxy groups available for hydrolysis and condensation. Because DPM and MPM monomers can only form oligomers with respectively M-/D- and M-structures (see Fig. 1), their ability to form cross links in the polymer structure of the shell is significantly reduced and so is the shell stiffness. For weakly cross-linked shells (MPM monomer, Fig. 3E) the droplets shrink almost freely during the polymerization yielding smaller spherical particles with a slightly corrugated surface. For higher cross-linking densities (DPM and TPM monomers Fig. 3D and 3C) the shells resist the droplets shrinkage and respond with a deformation. More specifically, DPM droplets crumple and buckle randomly whereas TPM droplets undergo a reproducible single buckling deformation giving the spherical cavities visible in Fig. 2 and 3C.

The facts that the initial oil-in-water emulsion can be prepared in bulk quantities by a robust and well-known nucleation and growth mechanism, and that the following polymerization causes the buckling of the oil droplets with 100% efficiency, ensure the high yield of this method and allow an easy scale up. We proved this point by preparing a 500 ml batch with 10% solids, which produced approximately 50 g of particles ($\sim 10^{13}$particles).

The reproducible and well-defined geometry of our buckled droplets allows them to be used as elementary building blocks in a lock-key assembly together with particles of complementary shape. We used spheres of different sizes and compositions, serving as the key particles, and the polymerized buckled droplets, serving as the lock particles. Depletion interactions caused by a dissolved non-adsorbing polymer were used to drive the assembly.[15]

Key particles were fabricated using well know methods[20,22,23] and comprise spheres of poly(methyl methacrylate), polystyrene and silica and ellipsoids of hematite (α-Fe_2O_3). All the particle used in the experiments were dispersed in water at a pH of 9 to ensure enough negative surface charge required for colloidal stability. A depletion attraction between the particles is introduced by dissolving poly-(ethylene oxide) (PEO) in a water mixture containing both lock and key particles. By a proper adjustment of the concentration and size of PEO, the strength of the depletion interaction can be adjusted to bind exclusively lock-key pairs (see Fig. 4). In our experiments we used PEO with a molecular weight of 600,000 and a concentration that varied between 0.4 and 0.9 g/L. Occasionally pNIPAM nanoparticles with a radius of 65nm (measured at 25 °C) were used as depletant to allow controlling the interaction using temperature.[15] For this experiment the lock particles were coated with a layer of polyacrylamide to avoid the adsorption of the depletant onto their surface. The coating was performed by polymerizing at 75 °C, 80 mg of N-isopropylacrylamide in 20 ml of an aqueous solution of KPS [0.1% w/w] in the presence of lock particles (typically $c_{lock} \leq 2\%$ w/w). Examples of lock-key assemblies are highlighted in Fig. 4. The

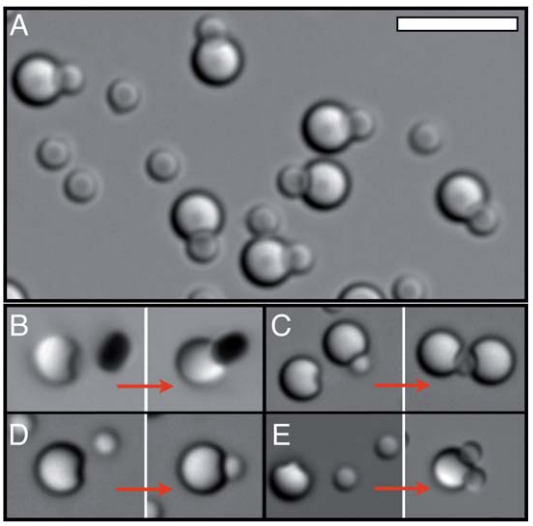

Fig. 4 (A) shows a microscopy picture of self-assembled lock-key pairs from a lock : key ratio of 1 : 2 and (B–E) show time sequences of binding events between locks and different complementary keys. Shape and composition of the key particles are varied: magnetic hematite ellipsoids in (B) and spheres of silica, PMMA and PS in (C), (D) and (E) respectively. The scale bar is 5 μm.

binding is entirely determined by the lock and key complementary geometry and does not depend on the surface chemistry of the particles. Thus, keys having identical shapes but different composition are interchangeable. Another important consequence of the absence of covalent bonds between lock and key is that they can be used to make colloidal aggregates whose shape is flexible. For example, if two locks with spherical cavities bind to a single spherical key (see Fig. 4C), a flexible ball-and-socket joint forms. More details on the lock and key interaction such as selectivity and reversibility are presented elsewhere.[15]

In conclusion, we have described how to fabricate particles with well-defined cavities *via* a simple, high yield method, based on a polymerization-induced buckling of monodisperse silicon oil droplets. The resulting organo-silica particles can be mixed with disparate types of colloids and reversibly assembled by depletion to form flexible clusters whose shape and composition can be programmed.

Acknowledgements

This work was supported partially by the National Science Foundation under Award Number DMR-0706453 and by the MRSEC Program of the National Science Foundation under Award Number DMR-0820341. S.S. was supported by the Netherlands Organization for Scientific Research (NWO) through a Rubicon fellowship. W.T.M.I. acknowledges support from Rhodia.

References

1 Y. Yin, Y. Lu, B. Gates and Y. Xia, *J. Am. Chem. Soc.*, 2001, **123**, 8718–29.
2 V. Manoharan, M. Elsesser and D. Pine, *Science*, 2003, **301**, 483–487.
3 D. Grier, *Nature*, 2003, **424**, 810–816.
4 G. A. DeVries, M. Brunnbauer, Y. Hu, A. M. Jackson, B. Long, B. T. Neltner, O. Uzun, B. H. Wunsch and F. Stellacci, *Science*, 2007, **315**, 358–361.
5 C. P. Lapointe, T. G. Mason and I. I. Smalyukh, *Science*, 2009, **326**, 1083–1086.
6 J. A. Fan, C. Wu, K. Bao, J. Bao, R. Bardhan, N. J. Halas, V. N. Manoharan, P. Nordlander, G. Shvets and F. Capasso, *Science*, 2010, **328**, 1135–1138.
7 S. Y. Park, A. K. R. Lytton-Jean, B. Lee, S. Weigand, G. C. Schatz and C. A. Mirkin, *Nature*, 2008, **451**, 553–556.
8 M. E. Leunissen, R. Dreyfus, F. C. Cheong, D. G. Grier, R. Sha, N. C. Seeman and P. M. Chaikin, *Nat. Mater.*, 2009, **8**, 590–595.
9 S. Jiang, Q. Chen, M. Tripathy, E. Luijten, K. S. Schweizer and S. Granick, *Adv. Mater.*, 2010, **22**, 1060–1071.
10 D. R. Breed, R. Thibault, F. Xie, Q. Wang, C. J. Hawker and D. J. Pine, *Langmuir*, 2009, **25**, 4370–4376.
11 H. Onoe, K. Matsumoto and I. Shimoyama, *Small*, 2007, **3**, 1383–9.
12 T. Clark, J. Tien, D. Duffy, K. Paul and G. Whitesides, *J. Am. Chem. Soc.*, 2001, **123**, 7677–7682.
13 C. Hernandez and T. Mason, *J. Phys. Chem. C*, 2007, **111**, 4477–4480.
14 G. Meng, N. Arkus, M. P. Brenner and V. N. Manoharan, *Science*, 2010, **327**, 560–563.
15 S. Sacanna, W. T. M. Irvine, P. M. Chaikin and D. J. Pine, *Nature*, 2010, **464**, 575–578.
16 T. Sugimoto, *Monodispersed particles*, Elsevier, 2001.
17 T. Obey and B. Vincent, *J. Colloid Interface Sci.*, 1994, **163**, 454–454.
18 C. Morin, L. Geulin, A. Desbene and P. Desbene, *J. Chromatogr.*, 2004, **1032**, 327–334.
19 A. Fery and R. Weinkamer, *Polymer*, 2007, **48**, 7221–7235.
20 R. Ottewill and J. Shaw, *Colloid Polym. Sci.*, 1967, **218**, 34–40.
21 C. Zoldesi and A. Imhof, *Adv. Mater.*, 2005, **17**, 924.
22 W. Stöber, A. Fink and E. Bohn, *J. Colloid Interface Sci.*, 1968, **26**, 62–69.
23 T. Sugimoto, M. Khan and A. Muramatsu, *Colloids Surf., A*, 1993, **70**, 167–169.

